Rare Gas Systematics in Popping Rock: Isotopic and Elemental Compositions in the Upper Mantle

Manuel Moreira, Joachim Kunz, Claude Allègre

New experimental data on the isotopic variations of neon, argon, and xenon in a popping rock imply that the $^{40}Ar/^{36}Ar$ ratio of the upper mantle is less than 44,000 and that the $^{129}Xe/^{130}Xe$ ratio is less than 8.2. The elemental abundance pattern of rare gases is chondritic-like and is quite distinct from the solar pattern. These data imply that Earth accreted from planetesimals that probably underwent a transformation of their rare gas budget from solar- to chondritic-like, leaving the isotopic composition unchanged from the solar pattern.

The rare gas content of material from Earth's upper mantle is extremely low and often reflects atmospheric contamination. The method for analyzing submarine basalts is to use glassy margins of lava flows erupted at great depth under the sea (*1*). Even in this case, the rare gas data mostly reflect contamination. However, a few samples permit more precise measurements because they have an exceptionally high gas concentration. One of these samples is the "popping rock" 2ΠD43. This sample has a high vesicularity (16 to 18%) and high gas concentrations (*2–5*). It was dredged in the North Atlantic at 13°46′N at a depth of 3510 m by the research vessel *Akademik Boris Petrov* in June 1985. Studies of rare gases in this popping rock have shown that the He isotopic ratio is similar to the mean mid-oceanic ridge basalt (MORB) $^4He/^3He$ ratio of 88,000 and that the $^{40}Ar/^{36}Ar$ is high, up to 28,000, which is one of the highest values measured for MORBs (*4*). Thus, the isotopic compositions show that this sample reflects best the upper mantle rare gas compositions (*6*). It also has a $^{13}C/^{12}C$ isotopic ratio ($\delta^{13}C$) of up to −3.7 per mil, which indicates that the gases in this sample are rather weakly fractionated and therefore may represent the degassed mantle (*5*). We made two independent analyses of all rare gas isotopes in this sample by stepwise crushing (*7*) (Table 1).

Because the He content in the atmosphere is very low, He is an excellent tracer for mantle sources and yields evidence for two distinct mantle reservoirs. The reservoir source of MORB has a rather constant $^4He/^3He$ ratio close to 88,000 and is typically identified as the upper mantle (*8*). The radiogenic signature of the MORB reservoir results both from outgassing (*6*) and the decay of U and Th, which increases the $^4He/^3He$ ratio. The source of most OIBs (oceanic island basalts) has a much lower $^4He/^3He$ (down to 25,000) (9) and indicates the existence of a less degassed, therefore ^3He-rich, reservoir thought to be located in the lower mantle.

Contamination of MORBs by atmospheric Ne, Ar, Kr, and Xe can be extremely extensive (up to 100%), and for a long time it prevented the discovery of ^{40}Ar and $^{129}Xe/^{136}Xe$ anomalies in MORBs. Neon can serve as the Rosetta stone for solving this problem because it has three isotopes, and because of its low abundance, only the ^{21}Ne content can be substantially changed in mantle rocks by nucleogenic production (*10*). Sarda and collaborators (*2*) showed that the $^{20}Ne/^{22}Ne$ ratio of the upper mantle is different from the atmospheric ratio (which has a "planetary" ratio of 9.8) and appears to be solar-like (13.8) (*11*). In a three-isotope Ne diagram, all the MORB samples fall on a straight line that is interpreted as reflecting mixing between the MORB reservoir and air. Honda and collaborators (*12*) found that glasses from Loihi seamount have a $^{20}Ne/^{22}Ne$ ratio of up to 11.4 and a three-isotope correlation line that is steeper than the MORB line. Following the same approach as for He, they concluded that the MORB mantle is more nucleogenic than the lower mantle because it is more degassed [higher (U+Th)/Ne ratio]. In other locations, the $^{20}Ne/^{22}Ne$ ratio also approaches the solar value ($^{20}Ne/^{22}Ne$ ratio up to 13.2) and supports this interpretation (*7*, *13–16*). These studies have shown that Ne is an excellent tracer of atmospheric contamination in basalts because the $^{20}Ne/^{22}Ne$ ratios of the two mixing end members are quite well constrained. The correlation of the $^{20}Ne/^{22}Ne$ ratios with ^{21}Ne anomalies directly quantifies the contamination of the nucleogenic component. However, this nucleogenic Ne component should correlate with radiogenic and fissiogenic components of the other rare gases. Thus, the contamination by atmospheric Ar and Xe can be also quantified by investigation of their correlations with Ne isotopic composition.

A solar $^{20}Ne/^{22}Ne$ ratio (13.8) is a reasonable upper limit for the mantle, but the actual mantle value could well be between a solar value and the highest MORB value measured so far. Our study and all MORB data obtained by stepwise heating (*17*) yield a maximum $^{20}Ne/^{22}Ne$ ratio of ~12.5. The data include analyses from all final steps of crushing of the sample 2ΠD43 (Fig. 1 and Table 1). This ratio may indicate that the MORB mantle has a $^{20}Ne/^{22}Ne$ ratio close to 12.5, as also proposed by Niedermann *et al.* (*18*). But because the origin of this value is not yet clear [whether there is nucleogenic production of ^{22}Ne (*10*, *18*) or injection of atmospheric noble gases in the mantle], we use a solar $^{20}Ne/^{22}Ne$ ratio (13.8) to

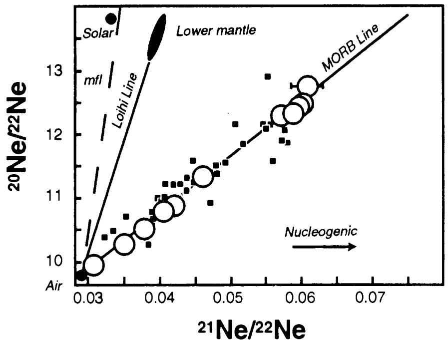

Fig. 1. Three-isotope Ne-Ne diagram showing the Ne results from the 2ΠD43 samples (circles). The black squares represent all the MORB samples (*17*). The Loihi line is from Honda *et al.* (*12*) and Valbracht *et al.* (*15*). The MORB line is from Sarda *et al.* (*2*). mfl indicates the mass fractionation line (dashed line). In all figures, error bars indicate 1σ uncertainty.

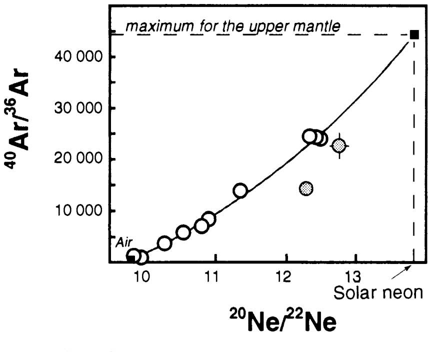

Fig. 2. $^{40}Ar/^{36}Ar$ ratio versus $^{20}Ne/^{22}Ne$ ratio from our MORB sample 2ΠD43. The best hyperbolic fit for a solar $^{20}Ne/^{22}Ne$ ratio is achieved for $r = 1.6 \pm 0.1$ and $^{40}Ar/^{36}Ar = 44,000$ in the upper mantle. The gray dots are not considered for the fit because of a problem of Ar blanks for these two analyses.

Université Denis Diderot-Paris 7, Laboratoire de Géochimie et Cosmochimie, Institut de Physique du Globe de Paris, CNRS Unité de Recherche Associée Number 1758, 4 Place Jussieu, 75252 Paris Cedex 05, France. E-mail: moreira@ipgp.jussieu.fr

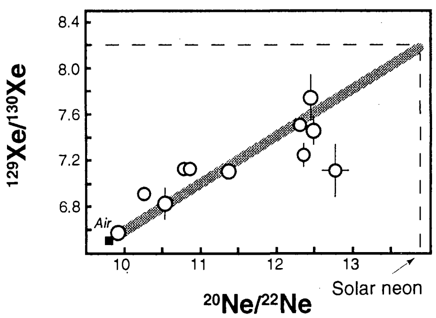

Fig. 3. ^{129}Xe/^{130}Xe ratio versus ^{20}Ne/^{22}Ne ratio from our MORB sample 2ΠD43. Heavy line, linear best fit; dashed line, maximum ^{129}Xe/^{130}Xe permitted in the upper mantle.

Table 2. ^{40}Ar/^{36}Ar, ^{129}Xe/^{130}Xe, ^{3}He/^{22}Ne, ^{3}He/^{36}Ar, ^{3}He/^{84}Kr, and ^{3}He/^{130}Xe ratios in the upper mantle, depending on its ^{20}Ne/^{22}Ne ratio (left column).

^{20}Ne/^{22}Ne	^{40}Ar/^{36}Ar	^{129}Xe/^{130}Xe	^{3}He/^{22}Ne	^{3}He/^{36}Ar	^{3}He/^{84}Kr	^{3}He/^{130}Xe
12.5	25,000	7.6	4.9	0.4	14.1	760
13.0	31,500	7.8	5.8	0.5	16.8	900
13.5	39,000	8.0	6.7	0.6	19.6	1040
13.8	44,000	8.2	7.3	0.7	21.3	1180

constrain the maximum ^{40}Ar/^{36}Ar and the ^{129}Xe/^{130}Xe ratios in the upper mantle.

Argon has three isotopes that could enable a deconvolution of mantle and atmospheric components similar to that used for Ne. However, it has not been demonstrated yet without ambiguity that the mantle ^{38}Ar/^{36}Ar signature is different from that of air (*19*). Thus, ^{40}Ar/^{36}Ar ratios and—for a similar reason—the Xe isotopic ratios ($^{129-136}$Xe/^{130}Xe) measured in MORBs are just lower limits, and estimates for the upper mantle composition have used the maximum measured values of 28,000 for the ^{40}Ar/^{36}Ar ratio and 7.5 for the ^{129}Xe/^{130}Xe ratio (*4*). Burnard *et al.* (*20*) expanded the range of ^{40}Ar/^{36}Ar ratios up to 40,000 by analyzing Ar from single vesicles of the same sample that we used for our present study. However, the authors proposed that all of the ^{36}Ar found still represents atmospheric contamination and suggested that the true mantle ^{40}Ar/^{36}Ar ratio could be up to 400,000.

Our new data on 2ΠD43 demonstrate a well-defined correlation between ^{40}Ar/^{36}Ar and ^{20}Ne/^{22}Ne (Fig. 2), which we interpret as resulting from mixing of the MORB component with an atmospheric component. In such a diagram, mixing is not represented by a linear relation but by hyperbola. The best fit for this hyperbola is given by $r = [^{22}\text{Ne}/^{36}\text{Ar}]_{\text{UM}}/[^{22}\text{Ne}/^{36}\text{Ar}]_{\text{air}}$ of 1.6 ± 0.1 (where r is the hyperbola parameter and UM indicates the upper mantle), and the maximum permitted ^{40}Ar/^{36}Ar ratio for the upper mantle is 44,000 if ^{20}Ne/^{22}Ne = 13.8 (Fig. 2). For the ^{129}Xe/^{130}Xe-^{20}Ne/^{22}Ne correlation, we obtain the result that ^{129}Xe/^{130}Xe in the upper mantle is at most ~8.2 (Fig. 3).

Our upper mantle ^{40}Ar/^{36}Ar ratio derived from Ne-Ar systematics is close to the highest measured ratios for single vesicles (*20*). However, this value may still be too high if we suppose that the upper mantle ^{20}Ne/^{22}Ne ratio can be lower than the solar value (Table 2), if some injection in the upper mantle of atmospheric Ne is possible, or if there is a nuclogenic production of ^{22}Ne (*18*).

The Ne systematics help also to estimate the rare gas elemental abundances of the upper mantle, because the correlations of ^{20}Ne/^{22}Ne and therefrom deduced ^{40}Ar/^{36}Ar and ^{129}Xe/^{130}Xe ratios can be compared with the elemental ratios ^{3}He/^{22}Ne, ^{3}He/^{36}Ar, and ^{3}He/^{130}Xe (Fig. 4). For the ^{3}He/^{84}Kr ratio, we used a ^{84}Kr/^{3}He-^{36}Ar/^{3}He correlation (Fig. 4C), because the mantle appears to have the same isotopic composition of Kr as the atmosphere. Using linear fits and assuming a solar ^{20}Ne/^{22}Ne, we obtain ^{3}He/^{22}Ne = 7.3, ^{3}He/^{36}Ar = 0.7, ^{3}He/^{84}Kr = 21.3, and ^{3}He/^{130}Xe = 1180 in the upper mantle. A lower-than-solar mantle ^{20}Ne/^{22}Ne ratio also gives lower elemental ratios (Table 2).

The ^{3}He/^{22}Ne ratio determined by our measurements is close to calculated ratios, assuming either a steady-state model for the upper mantle or that the upper mantle is in a closed system (*21*, *22*). This ratio indicates that this sample has unfractionated elemental ratios, as previously indicated by stable isotopes (*5*).

In a model of a degassed upper mantle and a lower, less degassed, mantle, the elemental ratios (^{3}He/^{22}Ne, ^{3}He/^{36}Ar, and so

Table 1. He, Ne, Ar, Kr, and Xe abundances (in cubic centimeters per gram at standard temperature and pressure) and isotopic ratios in the 2ΠD43 popping rock samples. ^{38}Ar/^{36}Ar ratios have considerable uncertainty and are indistinguishable (2σ level) from the atmospheric ratio (0.188). The times sign refers to the cumulative number of strokes. Numbers in parenthesis indicate a 1σ error in the last digits. Errors in abundance are 5% (1σ). NA, not analyzed.

	^{4}He (10^{-6})	^{22}Ne (10^{-10})	^{36}Ar (10^{-9})	^{84}Kr (10^{-11})	^{130}Xe (10^{-13})	^{4}He/^{3}He	^{20}Ne/^{22}Ne	^{21}Ne/^{22}^{22}Ne	^{40}Ar/^{36}Ar	^{129}Xe/^{130}Xe	^{136}Xe/^{130}Xe	^{4}He/^{40}Ar*
						Experiment 1						
(0.9414 g)												
5×	61	2.7	2.8	9.9	13	83,000 (970)	11.34 (4)	0.0460 (2)	13,800 (100)	7.09 (5)	2.39 (2)	1.63
10×	8.8	4.5	8.7	15	9.4	87,500 (1300)	9.94 (3)	0.0306 (1)	1,050 (3)	6.57 (6)	2.21 (2)	1.34
20×	12	0.96	1.6	3.3	3.1	87,500 (1400)	10.53 (4)	0.0376 (2)	5,700 (20)	6.83 (14)	2.30 (5)	1.35
30×	5.5	0.13	0.15	0.59	0.82	85,500 (1400)	12.44 (7)	0.0594 (8)	24,300 (100)	7.73 (23)	2.57 (10)	1.50
130×	4.3	0.10	0.12	0.47	0.69	84,700 (1700)	12.48 (7)	0.0599 (8)	24,000 (120)	7.44 (12)	2.50 (5)	1.52
Total	91	8.4	13	29	27	84,300	10.52	0.0371	4,700	6.91	2.33	1.54
						Experiment 2						
(1.4052 g)												
3×	34	24	48	120	100	87,500 (1100)	9.85 (2)	0.0295 (2)	800 (5)	6.55 (3)	2.22 (1)	1.43
6×	16	0.09	1.3	3.8	4.7	87,200 (1200)	10.89 (2)	0.0418 (3)	8,000 (100)	7.13 (4)	2.38 (1)	1.59
10×	17	1.1	1.5	4.1	5.0	88,200 (1200)	10.79 (2)	0.0403 (3)	6,000 (60)	7.12 (4)	2.39 (2)	1.71
15×	4.3	NA	0.28	0.94	1.2	92,100 (2400)	NA	NA	8,970 (260)	7.06 (6)	2.35 (3)	1.75
25×	4.8	0.14	0.22	0.65	1.1	85,300 (1100)	12.29 (2)	0.0569 (4)	14,00 (300)	7.50 (6)	2.51 (3)	1.57
50×	3.7	0.51	0.85	2.1	1.8	85,000 (1200)	10.26 (2)	0.0349 (2)	3,600 (30)	6.91 (6)	2.31 (3)	1.28
100×	2.0	0.05	0.06	0.27	0.45	85,300 (1200)	12.34 (4)	0.0586 (6)	24,500 (1700)	7.24 (10)	2.38 (5)	1.49
400×	0.38	0.01	0.01	0.06	0.11	86,100 (1200)	12.76 (18)	0.0607 (23)	22,400 (2700)	7.11 (22)	2.40 (9)	1.40
Total	83	27	52	130	120	87,500	9.95	0.0307	1,343	6.62	2.24	1.52

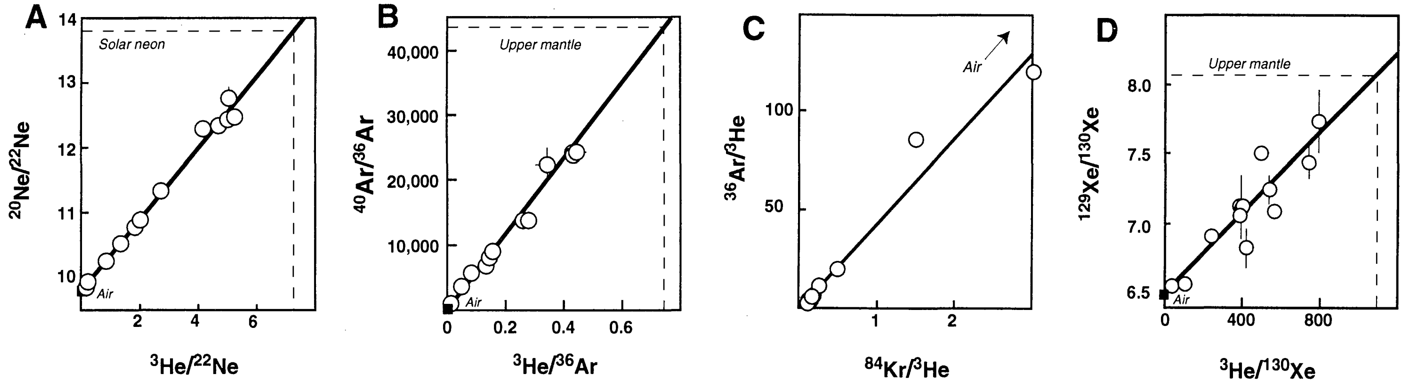

Fig. 4. (**A**) ^{20}Ne/^{22}Ne ratio versus the elemental ratio ^{3}He/^{22}Ne from our MORB sample 2ΠD43. (**B**) ^{40}Ar/^{36}Ar ratio versus the elemental ratio ^{3}He/^{36}Ar. (**C**) ^{36}Ar/^{3}He ratio versus ^{84}Kr/^{3}He ratio. (**D**) ^{129}Xe/^{130}Xe ratio versus the ^{3}He/^{130}Xe ratio. Two-component mixing is represented by a straight line because the same normalization isotope is used for the two axes in each figure.

on) should be equal in the two mantle layers as long as no elemental fractionation occured during outgassing of the upper mantle. This assumption has been verified by measurements of the ^{3}He/^{22}Ne ratio (*16*). To constrain the ^{3}He/^{36}Ar ratio in the lower mantle, a reliable estimate of ^{40}Ar/^{36}Ar in the lower mantle is needed. Suggestions for this ratio range from atmospheric values (or close to them) (*6*) up to a value as high as >15,000 (*13*, *22*, *23*). The ^{40}Ar/^{36}Ar ratios measured in Loihi seamount basalts, thought to best represent the lower mantle, have always been low (<5000). To quantify the atmospheric contamination in a magma chamber or during submarine eruption, Valbracht *et al.* (*15*) used the Ne-Ar systematics and restricted the ^{40}Ar/^{36}Ar ratio to between 2000 and 5000. This case implies that the lower mantle ^{3}He/^{36}Ar ratio is between 0.4 and 1.1, which is close to the upper mantle value that we estimate above (0.7). Values for lower mantle Xe cannot be derived from a similar approach, because no clear anomalies of ^{129}Xe/^{130}Xe have been observed in Loihi basalts (*15*). We will suppose here that the Xe isotopic ratios of the lower mantle are atmospheric, and that the ^{3}He/^{130}Xe ratio is the same as in the upper mantle. Thus, we have experimental evidence (except for Xe) that the abundance patterns of the lower and upper mantles are similar and that we can extend the results for the upper mantle to the whole mantle.

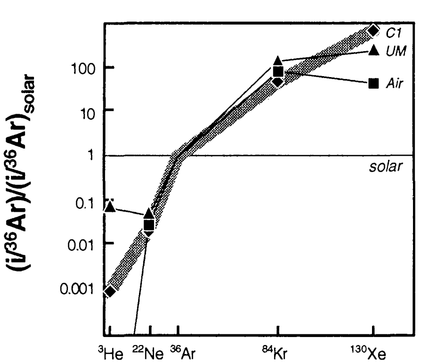

Fig. 5. Abundance of rare gases relative to ^{36}Ar, normalized to solar abundance $[(i/^{36}Ar)/(i/^{36}Ar)_{solar}]$ for the upper mantle (UM), atmosphere (air), chondrite C1 (C1), and solar-composition matter (solar) [from Table 2 and (*27*)].

Recently, Burnard *et al.* (*20*) suggested than the upper mantle rare gases have solar abundance patterns. This suggestion is essentially based on the assumption that the ^{3}He/^{36}Ar ratio is solar-like [they calculated a ratio of 1.4, whereas the solar ratio is 13; and they assumed that the ^{4}He/^{40}Ar* ratio is 3, which has not been proved: it seems to be 1.5 (Table 1) (^{40}Ar* is radiogenic ^{40}Ar, corrected for air contamination)]. If this model were correct, accretion would have been homogeneous with a complete loss of planetary rare gases from the planetesimals because of the high energies involved in the accretion process. The (proto-)Earth would then have acquired its mantle gas budget directly from the solar-like nebular gases, probably by solution in a magma ocean in equilibrium with a dense solar-like atmosphere that was blown off and lost quite early (*24*). In this scenario, an atmosphere such as we have now on Earth would have to be formed from a late volatile-rich veneer (*25*). Degassing of the Earth's interior should be negligible, except for the isotopes ^{4}He and ^{40}Ar, which are produced by radioactive decay in considerable quantities, and perhaps also the Ne isotopes, whose concentration in the atmosphere is likely to be a mixture of planetary and solar Ne values (*26*).

However, the normalization to ^{36}Ar and solar abundances (Fig. 5) demonstrates that the rare gas abundances in the upper mantle are similar to the planetary pattern of primitive chondrites (C1) (*27*) and distinct from the solar pattern. This observation justifies the application of models that explain the formation of Earth's atmosphere by mantle degassing (*6*, *27*, *28*).

On the other hand, it has been well established that a solar-like Ne isotopy is present in the mantle (*2*, *12*–*15*). Even if the He/Ne ratio appears also to be solar-like (as indicated by an almost flat pattern in Fig. 5), because the Ne/Ar ratio is planetary-like (Fig. 5), the solar-like He/Ne ratio simply reflects an excess of ^{3}He. Thus, we suggest that the materials that accreted to form Earth underwent a transformation of their rare gas abundances from solar- to planetary-like values. This elemental fractionation can be more easily achieved than an isotopic fractionation. For this reason, the isotopic ratios in Earth's interior remained solar-like. The debated existence of solar ^{38}Ar/^{36}Ar in the mantle (*15*) and the isotopic compositions of stable isotopes of Kr and Xe would support this suggestion (*29*). The excess of He in the mantle (compared to planetary values) may be a hint about the processes involved in the transformation from solar-like to planetary-like abundances, which should be linked to the different physicochemical behavior of He and the other rare gases. There are three important processes that may play a role: The light species, especially He, are more soluble in magmas and are more mobile by diffusion than the heavier ones, whereas they are less affected by adsorption (*30*, *31*).

The present Earth's atmosphere is a further-evolved rare gas reservoir. It resulted from solid Earth degassing and was probably subject to additional changes by trapping [sedimentary adsorption (*32*)], loss into space [hydrodynamic escape (*33*)], and remixing with late veener components [comets, for example (*26*)].

REFERENCES AND NOTES

1. J. Dymond and L. Hogan, *Earth Planet. Sci. Lett.* **20**, 131 (1973).
2. P. Sarda, T. Staudacher, C. Allègre, *ibid.* **91**, 73 (1988).

3. P. Sarda and D. Graham, *ibid.* **97**, 268 (1990).
4. T. Staudacher *et al.*, *ibid.* **96**, 119 (1989).
5. M. Javoy and F. Pineau, *ibid.* **107**, 598 (1991); F. Pineau and M. Javoy, *ibid.* **123**, 179 (1994).
6. C. Allègre, T. Staudacher, P. Sarda, M. Kurz, *Nature* **303**, 762 (1983); C. Allègre, T. Staudacher, P. Sarda, *Earth Planet. Sci. Lett.* **81**, 127 (1986/87).
7. The stepwise crushing (five steps and eight steps) and the measurements on two different mass spectrometers (ARESIBO I and ARESIBO II) were performed as decribed in M. Moreira, T. Staudacher, P. Sarda, J.-G. Schilling, C. Allègre, *Earth Planet. Sci. Lett.* **133**, 367 (1995).
8. T. Staudacher, M. Moreira, C. Allègre, *Mineral. Mag.* **58A**, 874 (1994); C. Allègre, M. Moreira, T. Staudacher, *Geophys. Res. Lett.* **22**, 2325 (1995).
9. H. Craig and J. Lupton, *Earth Planet. Sci. Lett.* **31**, 369 (1976); I. Kaneoka and N. Takaoka, *ibid.* **39**, 382 (1978); M. Kurz, W. Jenkins, S. Hart, *Nature* **297**, 43 (1982); T. Staudacher, M. Kurz, C.J. Allègre, *Chem. Geol.* **56**, 193 (1986); T. Staudacher, P. Sarda, C. Allègre, *ibid.* **59**, 35 (1990).
10. I. Yatsevich and M. Honda, *J. Geophys. Res.* **102**, 10291 (1997).
11. Rare gases in the solar system can be—in a first-order approach—subdivided into planetary, as found in chondrites and the atmospheres of the inner planets, and solar, as ejected from the sun in the solar wind and flares and implanted in the surface of orbiting objects such as meteoroids and the moon. The isotopic composition of Ne is distinct for these components. Solar Ne has a ^{20}Ne/^{22}Ne = 13.8 [J.-P. Benkert, H. Baur, P. Signer, R. Wieler, *J. Geophys. Res.* **98**, 13147 (1993)]. Planetary Ne is heavier, with ^{20}Ne/^{22}Ne = 8.5 [E. Mazor, D. Heymann, E. Anders, *Geochim. Cosmochim. Acta*, **34**, 781 (1970)], though it might be better represented by "phase-Q Ne," with ^{20}Ne/^{22}Ne = 10.7 (*29*).
12. M. Honda, I. McDougall, D. Patterson, A. Doulgeris, D. Clague, *Nature* **349**, 149 (1991).
13. R. Poreda and K. Farley, *Earth Planet. Sci. Lett.* **113**, 129 (1992).
14. M. Moreira, P. Valbracht, T. Staudacher, C. Allègre, *Geophys. Res. Lett.* **23**, 2453 (1996); P. Valbracht *et al.*, *Earth Planet. Sci. Lett.* **138**, 29 (1996).
15. P. Valbracht, T. Staudacher, A. Malahoff, C. Allègre, *Earth Planet. Sci. Lett.* **150**, 399 (1997).
16. M. Moreira and C. Allègre, *Chem. Geol.*, in press.
17. We have considered maximum ^{20}Ne/^{22}Ne ratios measured by Sarda *et al.* (*2*); H. Hiyagon, M. Ozima, B. Marty, S. Zashu, H. Sakai, *Geochim. Cosmochim. Acta* **56**, 1301 (1992); and unpublished data from our laboratory. One point from (*2*) with a ^{20}Ne/^{22}Ne ratio of 13.2 ± 1.0 was not considered because of its large uncertainty.
18. S. Niedermann, W. Bach, J. Erzinger, *Geochim. Cosmochim. Acta* **61**, 2697 (1997).
19. M. Ozima, *Rev. Geophys.* **32**, 405 (1994).
20. P. Burnard, D. Graham, G. Turner, *Science* **276**, 568 (1997).
21. We can write the equation

$$\left[\frac{^{21}\mathrm{Ne}}{^{22}\mathrm{Ne}}\right]_{\mathrm{MORB}} = \left[\frac{^{21}\mathrm{Ne}}{^{22}\mathrm{Ne}}\right]_{\mathrm{i}} + \left[\frac{^{21}\mathrm{Ne}^*}{^{4}\mathrm{He}^*}\right]\left[\frac{^{4}\mathrm{He}^*}{^{3}\mathrm{He}}\right]\left[\frac{^{3}\mathrm{He}}{^{22}\mathrm{Ne}}\right]$$

where (^{21}Ne/^{22}Ne)$_i$ is the initial ratio, (^{21}Ne/^{22}Ne)$_{MORB}$ is the MORB ratio (actual), (^{21}Ne*/^{4}He*) is the production ratio, and (^{4}He*/^{3}He) is the difference between the MORB ratio (~90,000) and the ^{4}He/^{3}He initial ratio [either 5000 (solar) or 20,000 (in the present lower mantle)]. If it is assumed that the upper mantle is a closed system (after the outgassing), (^{21}Ne/^{22}Ne)$_i$ = 0.0328 (solar), (^{21}Ne/^{22}Ne)$_{MORB}$ = 0.075, (^{21}Ne*/^{4}He*) = 4.5×10^{-8} (*10*) or 9×10^{-8} [T. Kyser and W. Rison, *J. Geophys. Res.* **87**, 5611 (1982)], and (^{4}He*/^{3}He) = 90,000 − 5000 = 85,000, we can estimate that the ^{3}He/^{22}Ne ratio is between 11 (^{21}Ne*/^{4}He* = 4.5×10^{-8}) and 5.5 (^{21}Ne*/^{4}He* = 9×10^{-8}), a value that is very similar to our measurements. These results are exactly the same in the case of an upper mantle in a steady state [(*22*); K. O'Nions and I. Tolstikhin, *Earth Planet. Sci. Lett.* **124**, 131 (1994); L. Kellog and G. Wasserburg, *Earth Planet. Sci. Lett.* **99**, 276 (1990)].
22. D. Porcelli and G. Wasserburg, *Geochim. Cosmochim. Acta* **59**, 4921 (1995).
23. B. Marty and P. Alle, in *Noble Gas Geochemistry and Cosmochemistry*, J. Matsuda, Ed. (Terra Scientific, Tokyo, 1994), pp. 191–204.
24. C. Harper and S. Jacobsen, *Science* **273**, 1814 (1996).
25. T. Owen, A. Bar-Nun, I. Kleinfield, *Nature* **358**, 43 (1992).
26. B. Marty, *Earth Planet. Sci. Lett.* **94**, 45 (1989).
27. R. Pepin, *Icarus* **92**, 2 (1991).
28. Review in M. Ozima and F. Podosek, *Noble Gas Geochemistry* (Cambridge Univ. Press, Cambridge, 1983), pp. 1–367; M. Ozima and K. Zahnle, *Geochem. J.* **27**, 185 (1993); I. Azbel and I. Tolstikhin, *Meteoritics* **28**, 609 (1993).
29. The isotopic composition of stable isotopes of Kr and Xe in Earth's atmosphere is different from their solar and planetary isotopic compositions (*28*). Although the origin of this fractionation is still debated (*27*), it may indicate that the evolution of these isotopic ratios is even more complicated than for He, Ne, and Ar, and that Kr and Xe are rather unsuitable for testing our model. They would also fail to serve as a test because their solar and planetary compositions show quite similar isotopic patterns (*28*). Finally, there is to our knowledge no evidence that the composition of stable isotopes of Kr and Xe in the mantle differs from that in the atmosphere, which may indicate the injection of some atmospheric Kr and Xe into the mantle as may have also happened for Ne and would explain the lower-than-solar ^{20}Ne/^{22}Ne ratio in the upper mantle.
30. R. Wieler, E. Anders, H. Baur, R. Lewis, P. Signer, *Geochim. Cosmochim. Acta* **55**, 1709 (1991).
31. J. Yangand and E. Anders, *ibid.* **46**, 877 (1982); J. F. Wacker, *ibid.* **53**, 1421 (1989).
32. F. Fanale and P. Cannon, *Earth Planet. Sci. Lett.* **11**, 361 (1971); F. A. Podosek, T. J. Bernatowicz, F. E. Kramer, *Geochim. Cosmochim. Acta* **45**, 2401 (1981).
33. D. Hunten, R. Pepin, J. Walker, *Icarus*, **43**, 22 (1987).

34. This is contribution number 1510 of the Institut de Physique du Globe de Paris. We thank P. Sarda, T. Staudacher, M. Javoy, F. Pineau, and P. Cartigny for discussions. The manuscript was improved by the comments of two anonymous reviewers.

27 October 1997; accepted 14 January 1998

The Formation of HCS and HCSH Molecules and Their Role in the Collision of Comet Shoemaker-Levy 9 with Jupiter

R. I. Kaiser,* C. Ochsenfeld, M. Head-Gordon, Y. T. Lee†

The reaction of hydrogen sulfide with ground-state atomic carbon was examined with crossed molecular beams experiments and ab initio calculations. The thiohydroxycarbene molecule, HCSH, was the reactive intermediate, which fragmented into atomic hydrogen and the thioformyl radical HCS. This finding may account for the unassigned HCS source and an unidentified HCSH radical needed to match observed CS abundances from the collision of comet Shoemaker-Levy 9 into Jupiter. In the shocked jovian atmosphere, HCS could further decompose to H and CS, and CS could react with SH and OH to yield the observed CS_2 and COS.

The discovery of comet D/Shoemaker-Levy 9 (SL9) initiated the only observation of the collision of two solar system bodies (*1*). From 16 to 22 July 1994, about 20 fragments of the split nucleus impacted into Jupiter causing enormous atmospheric disturbances (*2*, *3*). Earth-based observations detected large amounts of the sulfur-containing molecules S_2, COS, CS_2, CS, and H_2S, which are not indigenous to Jupiter's atmosphere (*4*–*6*). Generic reaction networks simulating the impact-induced sulfur chemistry suffered from the lack of laboratory data on products and intermediates in the H-C-S system and failed to quantitatively reproduce observed abundances of sulfur-containing species in Jupiter's atmosphere. To match the observed data qualitatively, impact models had to include postulated reactions involving transient species such as HCS and CH_2S in the form of thioformaldehyde (H_2CS) (*7*, *8*).

We present crossed molecular beams experiments and ab initio calculations on the reaction of ground-state carbon atoms, $C(^3P_j)$, with hydrogen sulfide, H_2S:

$$C(^3P_j) + H_2S(X^1A_1) \rightarrow H_2SC \tag{1}$$

$$\rightarrow HCS(X^2A') + H(^2S_{1/2})$$

$$\rightarrow HSC(X^2A') + H(^2S_{1/2}) \tag{2}$$

$$\rightarrow CS(X^1\Sigma^+) + H_2(X^1\Sigma_g^+) \tag{3}$$

$$\rightarrow CS(X^1\Sigma^+) + 2H(^2S_{1/2}) \tag{4}$$

Atomic carbon is formed in initial SL9 collision–triggered shock waves characterized by high temperature of up to 5000 K and might survive reentry of the impact

---

Department of Chemistry, University of California, Berkeley and Chemical Sciences Division, Lawrence Berkeley National Laboratory, Berkeley, CA 94720, USA.

*Present address: Academia Sinica, Institute of Atomic and Molecular Sciences, 1, Section 4, Roosevelt Road, Taipei, 116, Taiwan, Republic of China, and Department of Physics, Technical University Chemnitz-Zwickau, 09107 Chemnitz, Germany.

†Present address: Academia Sinica, Institute of Atomic and Molecular Sciences, 1, Section 4, Roosevelt Road, Taipei, 116, Taiwan, Republic of China.